

Non-equilibrium Goldstone phenomenon in tachyonic preheating

Sz. Borsányi*, A. Patkós † and D. Sexty‡

Department of Atomic Physics

Eötvös University, Budapest, Hungary

November 26, 2018

Abstract

The dominance of the direct production of elementary Goldstone waves is demonstrated in tachyonic preheating by determining numerically the evolution of the dispersion relation, the equation of state and the kinetic power spectra for the angular degree of freedom of the complex matter field. The importance of the domain structure in the order parameter distribution for the quantitative understanding of the excitation mechanism is emphasized. Evidence is presented for the very early decoupling of the low-momentum Goldstone modes.

1 Introduction

The aim of this investigation is to contribute to the systematic exploration of the transition from the inflationary evolution of the Universe to the standard cosmological regime. The numerical analysis was performed in a simple hybrid inflationary model, in which the inflaton is coupled to a complex scalar field [1, 2]. The equations of the fields and of the scale parameter of FRW-geometry were solved simultaneously. The characteristics of the transition was studied for a range of the couplings and initial conditions. All choices fulfill the cosmological constraints entailing sufficient number of e-foldings during inflation and the generation of density perturbations compatible with the measured CMBR anisotropy.

The present investigation is focused on the excitation of Goldstone modes. In the literature the decay of global cosmic strings is advocated as the main source of these particles [3, 4, 5, 6]. It will be demonstrated that in the period of tachyonic instability [7, 8] a dominant *direct* Goldstone generation takes place. The importance of Goldstone production was first emphasized by Boyanovsky *et al.* [9, 10] in a renormalized large- N approach to the quantum dynamics of the symmetry breaking in the $O(N)$ model. They have extended their investigation to the FRW geometry in the framework of the new inflationary scenario [11]. The present investigation is an extension of our previous study

*mazsx@cleopatra.elte.hu

†patkos@ludens.elte.hu

‡denes@achilles.elte.hu

of the classical $O(N)$ system in Minkowski metrics in Ref. [12] to the case of FRW geometry. In the present paper also the period of instability is treated classically. Although the time interval of the instability is rather short it is instructive to study the transition of the scale parameter of the Universe from the inflationary regime to a regime dominated by the mixture of weakly interacting species. The system evolves smoothly from radiation domination towards matter dominated expansion. We study the field dynamics under the continuous variation of the power characterizing the time dependence of the cosmological scale factor.

In hybrid inflationary scenarios the rolling inflaton triggers the condensation of a complex scalar field thought to be the matter field driving the GUT phase transition. The transition is accompanied by spinodal (tachyonic) instabilities, which occur for the radial (in the present case, $O(2)$ -invariant) modes. Rising radial (Higgs) modes excite on their turn the angular (Goldstone) modes. We refer to this phenomenon as the non-equilibrium Goldstone effect. The study of the excitation and evolution of these modes is particularly important, since it turns out that during the later expansion these are the Goldstone modes which dominate the energy density of the system.

After the tachyonic instability is stopped one observes an excess in the gradient energy density of the Goldstone degree of freedom relative to the corresponding kinetic energy density which is argued in [5] to be the signature for the occurrence of finite density of global strings. Evidence will be presented for the importance of topological configurations (domain walls and/or strings) in causing this difference, which is sustained over a considerable time interval. Also, a clean radiative equation of state (EoS) is found for the Goldstone degree of freedom after the virial equilibrium is reached. During the further evolution, however, a clear two-component separation was observed in the Goldstone power spectra. Low-(comoving)- k modes decouple from the equilibration processes fairly early and expand further as a non-interacting massless radiation with a frozen momentum distribution. High- k modes interact with the massive (Higgs- and inflaton) modes and tend toward thermal equilibrium characterized by a common kinetic temperature. The size of the decoupled comoving k -interval of the Goldstone excitations increases with time.

In section 2 we present the model and describe how the initial conditions for the numerical solution of the field equations were chosen. The most important features of the excitation process of Goldstone modes, shortly outlined in the previous paragraph, are described in section 3. There also a simple estimate will be given for the ratio of the direct Goldstone production relative to the energy contained in extended objects. The features and the limitations of a semi-analytical model for the excitation of the different modes is discussed in section 4. Section 5 is devoted to the discussion of the late-time expansion. Conclusions are summarized in section 6.

2 Selection of couplings and initial conditions

The system consists of the real (harmonic) inflaton field $\sigma(\mathbf{x}, t)$ and the complex matter field $\phi(\mathbf{x}, t)$, with negative squared mass and a quartic stabilizing $O(2)$ -invariant self-interaction. Their evolution is treated self-consistently assuming a spatially flat FRW space-time characterised by its dynamically determined scale function $a(t)$. Metric fluctuations are beyond the scope of the present study. The equations describing the field dynamics of the system are the following:

$$\begin{aligned} 0 &= \ddot{\sigma}(\mathbf{x}, t) + 3H\dot{\sigma}(\mathbf{x}, t) - \Delta\sigma(\mathbf{x}, t) + m_\sigma^2\sigma(\mathbf{x}, t) + g^2|\phi(\mathbf{x}, t)|^2\sigma(\mathbf{x}, t), \\ 0 &= \ddot{\phi}(\mathbf{x}, t) + 3H\dot{\phi}(\mathbf{x}, t) - \Delta\phi(\mathbf{x}, t) + m^2\phi + \frac{\lambda}{6}|\phi(\mathbf{x}, t)|^2\phi(\mathbf{x}, t) + g^2\sigma^2(\mathbf{x}, t)\phi(\mathbf{x}, t). \end{aligned} \quad (1)$$

The FRW equation has the following form:

$$H^2 - \frac{8\pi}{3m_{pl}^2} \left[\frac{3m^4}{2\lambda} + \frac{1}{2} \left((\dot{\sigma}(\mathbf{x}, t))^2 + |\dot{\phi}(\mathbf{x}, t)|^2 \right) + \frac{g^2}{2} |\phi(\mathbf{x}, t)|^2 \sigma^2(\mathbf{x}, t) + \frac{1}{2} \left(m_\sigma^2 \sigma^2(\mathbf{x}, t) + m^2 |\phi(\mathbf{x}, t)|^2 \right) + \frac{\lambda}{24} |\phi(\mathbf{x}, t)|^4 \right] = 0. \quad (2)$$

In Eqs. (1) and (2) the Hubble parameter $H = \dot{a}(t)/a(t)$ was introduced, m_{pl} is the Planck-mass. In the second term of the left hand side of Eq. (2) the expression in the square brackets represents the microscopical energy density of the fields.

The field equations were rewritten in conformal time ($d\eta = dt/a(t)$) and then discretized in a comoving volume $(L/a(t))^3$, with $L = N\delta x a(t)/a(t_e)$, $N = 64, 128$, $|m|\delta x = 1$. Here t_e is the time instant where we start the solution of Eqs. (1) and (2), which has been conveniently choosen to slightly preceed the exit point from the inflation. In the plots to be presented below the time is measured relative to t_e .

For a stable solution one had to choose the ratio of the conformal time step $\delta\eta$ to the spatial lattice spacing δx in the range $1/16 - 1/64$. In the following we always use the powers of $|m|$ as units of measurement.

On the other hand we find for the physical extent of our system $N\delta x a(t)/a(t_e) \ll H^{-1}$. Therefore we actually study only a small portion of the volume of the whole Universe. This is different from the choice of the lattice spacing in Ref. [13], where the system is at least as large as one Hubble volume. Therefore we do not expect the string part of the Goldstone dynamics to be described truly faithfully, but the propagating quasiparticle excitations are well represented in the simulations.

In the investigation of the early appearance of Goldstone modes, the effect of the cut-off will not cause any finite lattice spacing distortion. The choice of the lattice constant is significant for the decay of the Higgs waves into Goldstone excitations. This process is energetically allowed as long as

$$M_{\text{Higgs}} \leq 2k_{\text{cut-off}}/a(t), \quad (3)$$

where $k_{\text{cut-off}}$ is the maximal allowed comoving momentum for the Goldstone waves on the lattice. With increasing redshift one arrives at an artificial stabilisation of the Higgs-waves, which can be pushed farther by using finer lattices.

The evolution of the matter field started in the symmetric phase, very close to the point $\phi_0(t_i) \equiv V^{-1} \int d^3x \phi(\mathbf{x}, t_i) = 0$, while the inflaton field was set to $\sigma_0(t_i) \equiv V^{-1} \int d^3x \sigma(\mathbf{x}, t_i) = m_{pl}$. The initial velocities are $\dot{\phi}_0(t_i) = \dot{\sigma}_0(t_i) = 0$. Here t_i denotes the initial instant of the inflation.

Two important cosmological constraints are to be satisfied. The first requires at least $N_{\text{TOT}} \sim 60$ e-foldings of the scale factor before the critical inflaton field value is reached which terminates the inflationary period. The other constraint stems from the relation of the quantum fluctuations of the inflationary period to the density fluctuations measured by the COBE experiment [14]. They restrict the allowed range of couplings $g^2, \lambda, m^2, m_\sigma^2$. In this investigation the GUT-scale was chosen for the scale of the end of inflation. Therefore for the quantity $m_{\text{Higgs}}^2 \equiv -2m^2$, variation in the region $m_H \sim 10^{(14-15)}$ GeV was allowed. The inflaton-Higgs coupling was varied in the interval $g = 0.01 - 0.1$. The value of the Higgs self-coupling was fixed with the relation $\lambda = 3g^2$, which is valid if the couplings of the hybrid theory are derived from a superpotential [15, 16].

The numerical method of selecting the couplings without relying on the slow-roll approximation was described in some detail in Ref. [17]. For the present investigation we have chosen $g = 0.1, m_H =$

$8.8 \times 10^{14} \text{GeV}$, $m_\sigma = 4.2 \times 10^{11} \text{GeV}$, $N_{TOT} = 60$ and $g = 0.01$, $m_H = 5.5 \times 10^{14} \text{GeV}$, $m_\sigma = 1.4 \times 10^{12} \text{GeV}$, $N_{TOT} = 60$. These points fulfill also the COBE constraint: $\delta\rho/\rho|_{COBE} \approx 5 \times 10^{-4}$, at say, $\Delta N_{TOT} = 5$ e-foldings before the start of the tachyonic instability. It turned out that for $g = 0.01$ the inequality (3) was violated very early, practically before the saturation of the tachyonic instability. Therefore most of our discussion relies on the analysis of the $g = 0.1$ case.

For the homogenous inflaton mode the amplitude and velocity values corresponding to the moment $t = t_e$ were taken over from the solution of the equations describing its roll-down. The absolute values of the amplitudes and of the canonical momenta of all inhomogenous modes were chosen to correspond to the quantum vacuum state e.g.:

$$\begin{aligned}\sigma_k(t_e) &= \sqrt{\frac{L^3}{2\omega_\sigma}} e^{i\alpha_k}, & \dot{\sigma}_k(t_e) &= -i\sqrt{\frac{L^3\omega_\sigma}{2}} e^{-i\alpha_k}, & \omega_\sigma^2 &= k^2 + m_\sigma^2, \\ \phi_k(t_e) &= \sqrt{\frac{L^3}{2\omega_\phi}} e^{i\beta_k}, & \dot{\phi}_k(t_e) &= -i\sqrt{\frac{L^3\omega_\phi}{2}} e^{-i\beta_k}, & \omega_\phi^2 &= k^2 + m^2 + g^2\sigma^2(k=0, t_e).\end{aligned}\quad (4)$$

The initial phases α_k, β_k were chosen randomly. The classical evolution would further decrease these magnitudes below the zero point quantum values as a result of the expansion of the universe, but the spinodal instability injects considerable excitation into them.

3 Direct Goldstone excitation via spinodal instability

The independent degrees of freedom. The time evolution of the normalized cross-correlation matrix introduced in [12] presents evidence that directly after the spinodal instability is over, one can choose for the three independent degrees of freedom characterizing the system the inflaton, the radial O(2) invariant motion of $r(\mathbf{x}, t) = |\phi(\mathbf{x}, t)|$ and the angular oscillations $\varphi(\mathbf{x}, t)$, ($\phi = r e^{i\varphi}$). The time evolution of the dispersion relation characterizing these degrees of freedom was calculated from the definition

$$\omega_k^2 = \frac{|\dot{X}_k|^2}{|X_k|^2}, \quad X_k = \sigma_k, r_k, (e^{i\varphi})_k, \quad (5)$$

and extrapolated to $k = 0$ for finding the corresponding masses [12, 17]. One obtains mass values for the angular phase factor shortly after the spinodal instability values which are compatible with zero within the error of the mass determination. This observation justifies the term “Goldstone” for the angular modes. In the following the radial degree of freedom will be simply referred to as Higgs, and the angular component as Goldstone.

The phase transition triggered by the inflaton field can be clearly seen on the time-evolution of the Higgs field $r(x, t)$ well characterized by its homogeneous mode $\bar{r}^V(t)$. There the tachyonic instability leads to an almost instantanous exponential switch into the symmetry broken regime as shown in Fig. 1. The Higgs field triggers the rise of the gradient energy of the Goldstone component with a slight delay and the increase of the Goldstone kinetic energy starts with a further delay. The sharp increase in the radial component is terminated by an oscillatory period, whose frequency is determined by the sum of the classical mass square around the minimum r_0 of the potential and the space average of the Higgs fluctuations: $-2m^2 + \lambda \bar{r}^V/2$, which is often referred to as the Hartree mass. It is clear from the figure that the oscillations in the Goldstone kinetic and gradient energies follow the same frequency.

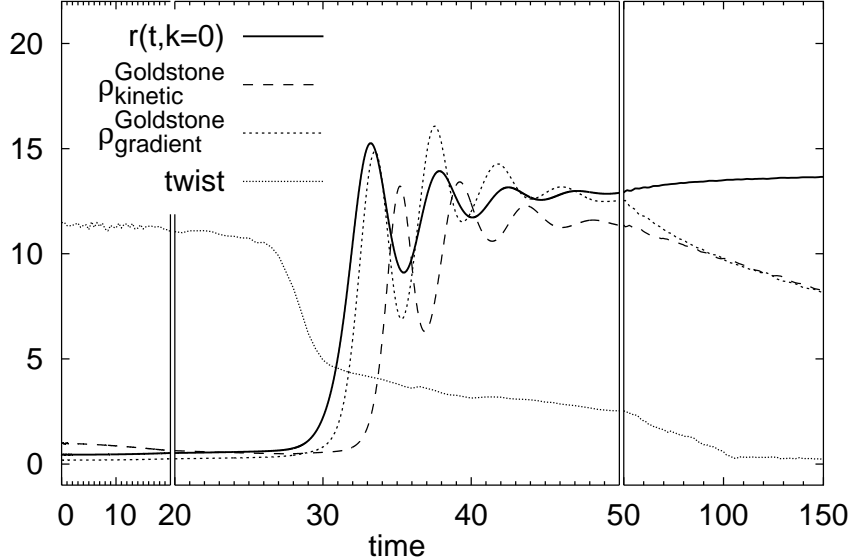


Figure 1: Virialization of the Goldstone oscillations, and the evolution of the average of the integrated twist in $\varphi(\mathbf{x}, t)$, calculated along straight lattice lines parallel to one of the axes. The oscillations of the radial field $\overline{r(\mathbf{x}, t)}^V$ tune the variation of the gradient and kinetic energy densities of the Goldstone modes ($g = 0.1$, $\lambda = 3g^2$, $N = 64$).

In Fig. 2 we analyze the time dependence of the temperatures calculated from the kinetic energies. It is the kinetic temperature of the Higgs component which starts to increase first reflecting the instability. Both the inflaton and the Goldstone kinetic temperatures follow it with approximately equal delay. This also hints to an excitation mechanism for these modes driven by the temporal variation of the Higgs field $r(\mathbf{x}, t)$ (see section 4). Fig. 2 also suggests that for $g = 0.1$ the three motions are apparently decoupled from each other for a short time interval ($|m|t \leq 100$) after the out-of-equilibrium oscillations are damped, each having its own nearly constant kinetic temperature.

The Goldstone field stays at the highest temperature $\sim (26 - 28)|m|$, which is slightly higher than the one-loop estimate of the critical temperature $\sqrt{72/(N_{comp} + 2)\lambda}|m| \sim 24.5|m|$, for an $O(N_{comp} = 2)$ model, with $\lambda = 0.03$. The other two degrees of freedom are much colder. Instant “freezing” characterizes the behavior of the inflaton field. It obtains a rather large squared mass, nearly equal to the Higgs mass, due to the supersymmetric $\lambda - g^2$ relation (e.g. $m_\sigma^2 - 6g^2m^2/\lambda \approx -2m^2 = m_{\text{Higgs}}^2$), therefore the amplitude of its oscillations becomes very small. One calculates the potential energy of the inflaton with its “new” mass when checking the virial equilibrium in this degree of freedom. The sudden increase of its energy density can be understood to be the result of this mass change (see section 4).

On the right hand end of Fig. 2 the effect of the late-time expansion appears: the temperature of the inflaton field is hardly varying which corresponds to its non-relativistic nature. On the other hand the temperature-ratio of the Higgs and the Goldstone fields stays nearly constant for $t \leq 5000$. We shall return to the discussion of the coupled cooling of the radial and of the angular $O(2)$ components in section 5.

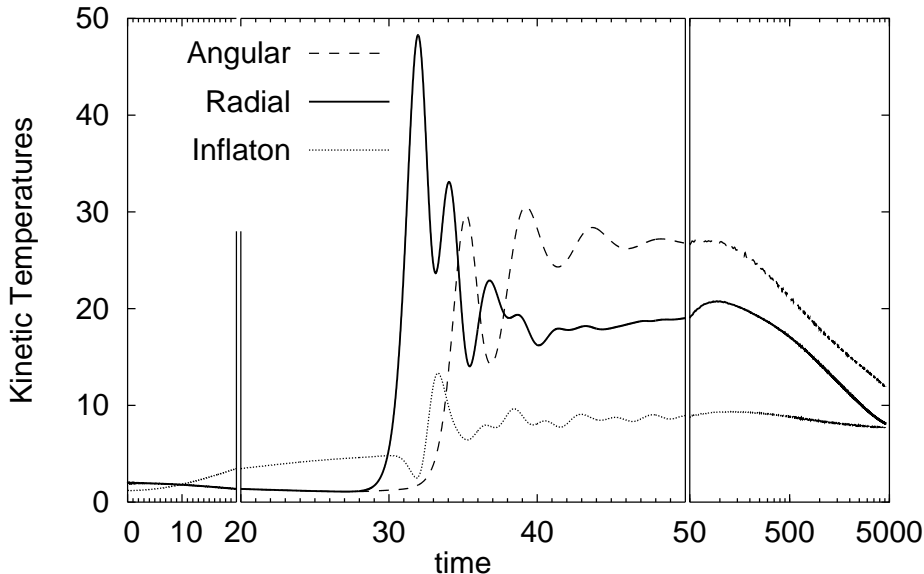


Figure 2: Kinetic temperatures of the independent degrees of freedom ($g = 0.1, \lambda = 3g^2, N = 64$). The figure represents the average of 16 runs starting with random initial phases.

The equations of state. We observed that the system stays in a rather stable way deep in the broken symmetry phase, despite the fact that the Goldstone temperature is high. One might attempt in such circumstances to characterize each species as a noninteracting gas, possessing its own equation of state.

In Fig. 3 the EoS of all three degrees of freedom are shown. It is clear, that they possess an EoS from rather early times, promptly after the large amplitude $r(t, \mathbf{x})$ oscillations are damped. They are nearly linear, of the form $p = w\rho$. The cooling pushes the system through the points of the EoS at the pace of the expansion, therefore the different points can be labeled by the instant when the system passes through them. The initial period is determined by the motion of the homogenous inflaton and Higgs fields, therefore it is not surprising that the temporal labeling is almost independent of the random initial phases introduced in Eq. (4), specifying different runs.

The inflaton and the Higgs field have nearly the same mass of the order of the GUT-scale. Therefore we expect them (after the virial ‘‘equilibrium’’ is reached) to follow the same $p - \rho$ smooth line, with the decrease of the energy density due to the expansion. Since the inflaton is almost decoupled one expects for it $w \approx 0$, and finds at early times $w \sim 1/10$. The Higgs field starts with a slightly larger slope, and both species smoothly approach the non-relativistic $p = 0$ curve on a longer time scale.

The Goldstone oscillations obey after virialisation a perfect radiative EoS ($p = w\rho, w \approx 1/3$). For larger energy densities ($\rho \geq 20$), that is for earlier times, one observes a slight deviation from the slope $1/3$. The same evolution may be followed as a function of time in Fig. 1. The gradient energy grows higher than the kinetic energy as the Goldstone field gets excited. We refer to this delayed onset of the virial equilibrium as the period of gradient excess. This excess is mainly the result of the formation of topologically characterizable extended objects, that temporarily slow down the ordering

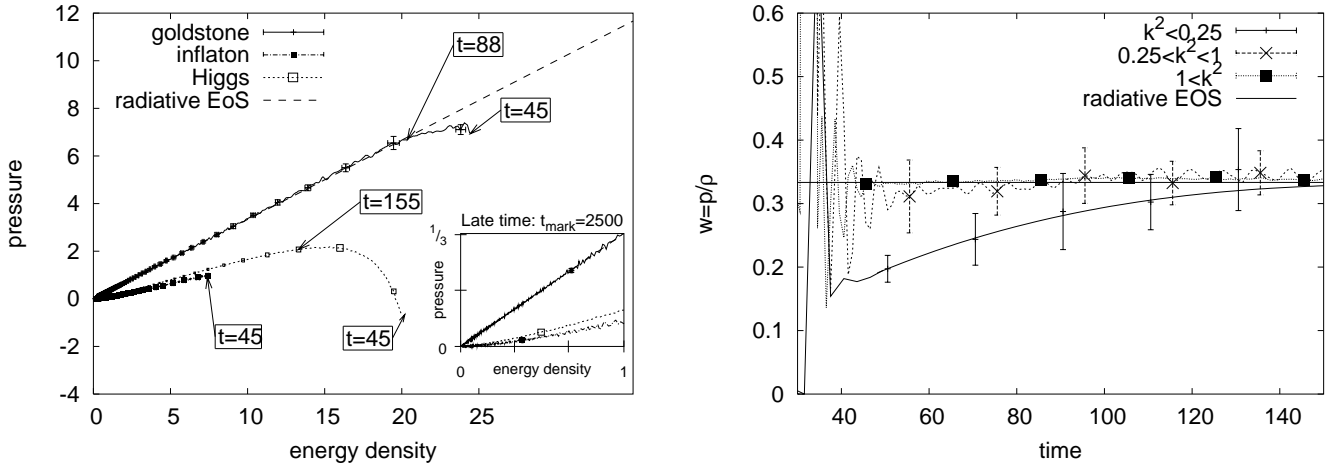


Figure 3: Equations of state (EoS) for the independent degrees of freedom ($g = 0.1, \lambda = 3g^2, N = 64$). In the left figure the $p(\rho)$ trajectories are shown for the three independent degrees of freedom. The characteristic moments of time, where the linear regime, characterised by the constant $w = p/\rho$ sets in are indicated next to the curves and can be compared with Fig. 2. In the insert the EoS trajectories traversed by the system at late times are displayed. In the right figure the evolution of the EoS of the Goldstone oscillators in three different Fourier regions is shown. The curves show the average over 8 runs, the calculated standard deviations are displayed by the error bars. On the right hand side the roughness of the mean curves was smoothed out, consistently with the size of their standard deviations.

of the system. The lattice size we used ($N = 64$) already enables us to give a quantitative description of the gradient excess which is independent of the random initial conditions. Its late-time behaviour is affected, however, by a substantial finite volume dependence [13].

In order to understand the role played by these topological objects we separate their contribution to the energy density from the energy fraction carried by the ‘‘elementary’’ Goldstone quasiparticles. First we perform a spectral analysis by making use of the separation of length scales of the topological objects and of the quasiparticles. In our second approach we separate these two energy carriers by their different equations of state.

We expect the heavy objects to contribute only in the low k -region of the Fourier space. To see this, the k -space of the Goldstone motion was splitted into three characteristic regions: $k^2/|m|^2 = [(0, 0.25), (0.25, 1.0), (1.0, k_{\text{cut-off}}^2)]$. Separate EoS were fitted in the three regions. In the right figure of Fig. 3 one sees that the deviation from the radiative EoS is localised to the lowest k region. (The curve is rather insensitive to the exact choice of the value of the separating wave number). This is in agreement with the expectation that the deviation is caused by extended solitonlike objects (mainly strings). These objects are heavy, their mass per length should be of the order of the Higgs mass.

This separation allows a simple quantitative estimate for the composition of the ‘‘Goldstone gas’’, if one assumes that it consists of a noninteracting mixture of elementary massless Goldstone particles and of nonrelativistic heavy objects. We can restrict the analysis to the lowest k -region since in the two higher ones the EoS reflects the exclusive presence of elementary Goldstone particles. The measured (partial) ratio $\rho/p|_{\text{low}k}$ is given then by $3(1 + y)$, $y = \rho_{\text{heavy}}/\rho_{\text{elementary}}$. At $t|m| = 50$ we find for example $y \sim 2/3$, which smoothly approaches zero around $t|m| \sim 100$, till when the decay

of the heavy extended objects will be complete on the $N = 64$ lattice.

In order to compare the energy portion carried by the heavy objects to the full angular energy density we extend the previous analysis to the full momentum range. The time dependence of the ratio $\rho_{\text{heavy}}/\rho_{\text{full Goldstone}}$ may be fitted by an exponential decay with a rate of $19(1) |m|^{-1}$. This fit is restricted to the range between $45 < t|m| < 100$ where the EoS is already well defined and the energy density of the heavy objects is above the noise level. We expect that these topological objects were created during the tachyonic instability, hence at the time the EoS is stabilized some of them might have been decayed already. As an estimate for the initial topological energy density we extrapolated the exponential time dependence back to the moment of the instability and found that (for $N = 64$) no more than one third of the angular energy was concentrated in heavy objects and two thirds were carried by massless quasiparticles. This analysis substantiates our claim that direct Goldstone production dominates in the tachyonic preheating.

We close this section by remarks on the behavior of two complementary "diagnostics" of the evolution of the system. In Fig. 1 we also show the average of the integral of $\delta\varphi(x)$, which is the variation of the angular orientation of the complex field from one site to the next one along straight lines parallel to the three axes. This integral is very large before the instability. After a sudden drop suffered at the moment of the tachyonic instability, it continues to decay gradually. This evolution goes parallel with the disappearance of the gradient energy excess. The average time of virialisation increases with decreasing λ .

The evolution of topological defects in the angular component is only weakly reflected by the concentration of hot spots, i.e. lattice sites with small radial field values ($r < v/2$, with v being the classical expectation value of the Higgs field). The hot spot concentration drops almost two orders of magnitude during the spinodal instability. This experience is rather different from the findings in Ref. [18], where the couplings $g = 0.01, \lambda = 0.01$ were used.

4 On the mechanism of tachyonic particle production

In hybrid inflationary scenarios the possible mechanisms for the Higgs field excitation were already discussed at length in the literature [15, 16, 18]. In this paper we concentrate on the angular component of the matter field and on the inflaton.

The excitation of the Goldstone and the inflaton field is driven by the Higgs field. It turns out that the gradient energy density of $r(\mathbf{x}, t)$ is about five times smaller than its kinetic energy density during the instability interval, therefore it is reasonable to replace $r^2(\mathbf{x}, t)$ in the field equations of the Goldstone and of the inflaton fields by its spatial average.

The analysis is particularly simple for the inflaton, because in this approximation the equations of its spatial Fourier components are linear. According to the proposed model the symmetry breaking simply increases the effective squared masses of these uncoupled oscillators:

$$\ddot{\sigma}_{\mathbf{k}} + \omega_{\mathbf{k}}^2(t) \sigma_{\mathbf{k}} = 0, \quad \omega_{\mathbf{k}}^2(t) = \mathbf{k}^2 + m_{\sigma}^2 + g^2 \bar{r}^2(t). \quad (6)$$

Since we are interested in the excitation mechanism, which is rather unaffected by the overall expansion ($H^{-1} \gg \Delta t_{\text{reheating}}$) we dropped the derivatives of the scale factor in these equations.

One can construct the energy balance of each mode:

$$E_{\mathbf{k}}(t) - E_{\mathbf{k}}(0) = \frac{g^2}{2} \int_0^t dt' \frac{d\bar{r}^2(t')}{dt'} \sigma_{\mathbf{k}}^2(t'), \quad E_{\mathbf{k}}(t) = \frac{1}{2}(\dot{\sigma}_{\mathbf{k}}^2 + \omega_{\mathbf{k}}^2(t) \sigma_{\mathbf{k}}^2). \quad (7)$$

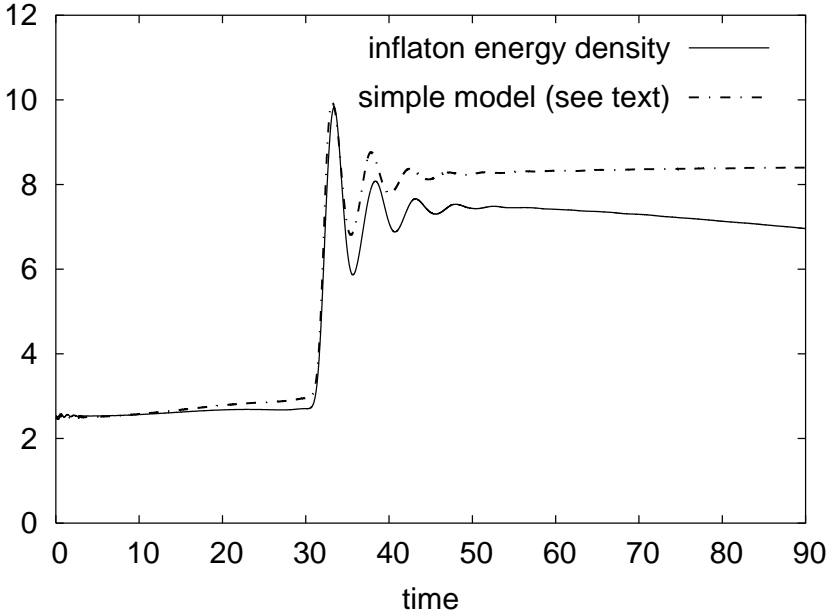


Figure 4: Comparison of the evolution of inflaton's energy density with the result of the simple model of independent oscillators based on the symmetry breaking induced variation of the inflaton mass (an average over 16 runs is displayed, $g = 0.1, N = 64$)

If one sums up the equations for all \mathbf{k} , one finds

$$E_{\text{inflaton}}(t) - E_{\text{inflaton}}(0) = \frac{g^2}{2} \int_0^t dt' \frac{d\overline{r^2}^V(t')}{dt'} \overline{\sigma^2}^V(t'). \quad (8)$$

This result may be easily compared to the full numerical solution. Inserting on the right hand side the measured quadratic fluctuations of the inflaton and the Higgs field one generates the dashed curve in Fig. 4. The agreement is quite spectacular, giving strong support to the proposed excitation mechanism. The deviation on the right half of the plot is due to the expansion we have neglected in this simple model, since the act of the excitation was in the focus of our interest.

A similar approximate construction might be attempted for the Fourier transform of the angular variable, which leads to the equation:

$$\ddot{\varphi}_{\mathbf{k}}(t) + 2 \frac{d}{dt} \overline{\ln r(\mathbf{x}, t)}^V \dot{\varphi}_{\mathbf{k}} + k^2 \varphi_{\mathbf{k}} = 0, \quad (9)$$

where the upper index means spatial averaging. This is a set of equations for independent oscillators damped by a common friction. Both the friction coefficient $\frac{d}{dt} \overline{\ln r(\mathbf{x}, t)}^V$ and the initial conditions for $\varphi_{\mathbf{k}}$ were taken from the numerical solution of the full dynamics. An equation like Eq. (9) could in principle account for the delay in the excitation of the Goldstone kinetic energy (see Fig. 1) since the short but strong common friction effect provides for the initially independent angular oscillation modes a common phase by nearly stopping all of them ($\dot{\varphi}_{\mathbf{k}} \approx 0$) in the same instant.

The energy density resulting from the solution of Eq. (9) produced much less excitation in the Goldstone modes than one observes in the full solution of Eq. (1) for any choice of the starting time

for Eq. (9). This forces us to conclude that the inhomogeneity of $r(\mathbf{x}, t)$ plays important role in the Goldstone excitation. The solution of Eq. (9) for low momenta approximately reproduces the spectral power of the full solution. The failure of the approximation is caused mainly by overestimating the damping of the high- \mathbf{k} modes. (An important effect possibly counter-balancing this overdamping will be discussed in section 5.) Calculations of the production rate of different elementary fields based on a homogenous Higgs field varying in time [19, 20] might underestimate the rate of the process of Goldstone quasiparticle production and overestimate in this way the fraction of heavy objects. This conclusion seems to depend rather sensitively on the value of the couplings λ, g^2 . The smaller is λ the more important is the inhomogenous contribution to the Higgs kinetic spectra already in the first oscillation period after the spinodal instability.

5 Expansion and late-time cooling

The variation of the cosmological scale factor settles directly after the instability at a rate reflecting radiation domination. We find by a high quality power law fit to its numerical evolution the behavior

$$a(t) \sim (t - \text{const.})^\gamma, \quad \gamma = 0.54(2), \quad (10)$$

where the error is estimated from the standard deviation of the fitted γ values when the time interval $t|m| = 50 - 2000$ is splitted into several shorter intervals. This exponent, however, shows a time dependence on longer time scales as it approaches $\gamma_{\text{matter}} = 2/3$.

This experience shows that special care must be taken if one wishes to enforce a simple power law behavior for $a(t)$ over an extended time interval as it was done in Refs. [5, 6, 18]. The exponent should be estimated from the energy contribution of the different degrees of freedom, and the result might be sensitive to the length of the time interval considered.

If the equations of state are linear, then the actual rate of expansion conforms to the equation of state of the mixture system:

$$\begin{aligned} p_{\text{full}}(t) &= w_{\text{full}}(t)\rho_{\text{full}}(t) \\ \gamma(t) &= \frac{2}{3(1 + w_{\text{full}}(t))}. \end{aligned} \quad (11)$$

This w_{full} coefficient is a subject of continuous shift from $w_{\text{full}} \approx 0.23(1)$ towards zero, which would mean the ideal matter dominated EoS. For the time interval of the fit Eq. (10) the time-averaged value $\overline{w_{\text{full}}} = 0.21(4)$ agrees well with the fitted γ exponent.

For completely decoupled field components one would expect

$$3(1 + w_i(t)) = -\frac{d \ln \rho_i(t)}{d \ln a(t)}, \quad i = \text{Goldstone, Higgs, inflaton} \quad (12)$$

with a time-independent w_i value, which should agree with the coefficients in the component-by-component EoS.

Indeed, this is the case of the inflaton, but the $O(2)$ sector shows rather large deviations. It turns out that the Goldstone energy density on the average decreases more slowly than expected for a massless radiation: $\rho_{\text{Goldstone}} \sim a^{3.59(1)}$. On the other hand the rate of cooling of the Higgs mode is faster than for a non-relativistic gas: $\rho_{\text{Higgs}} \sim a^{3.85(2)}$. The powers vary with time quite strongly. The

values above refer to an average over the $t|m| \in [500, 4500]$ interval. This indicates an energy transfer to the angular motion from the radial one, which terminates only when the matter domination era sets in ($t|m| \geq 5000$).

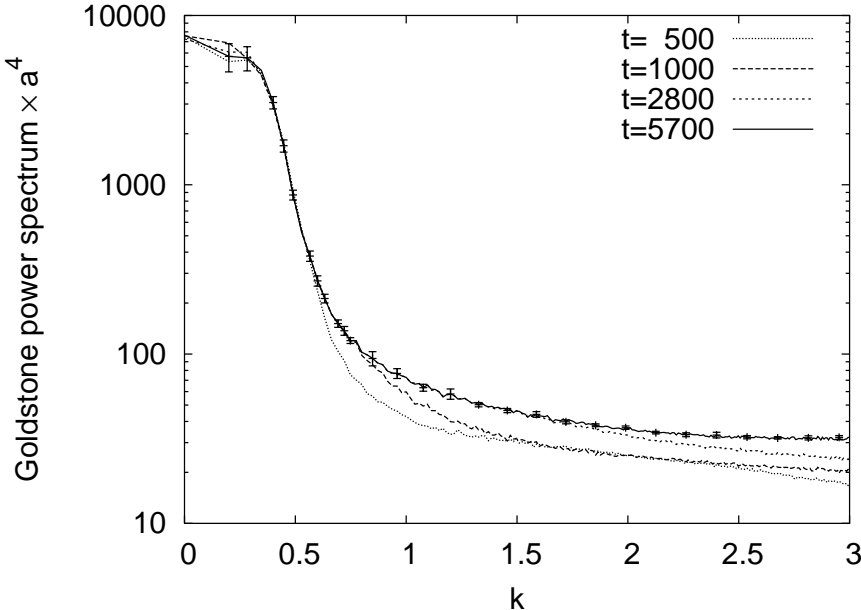


Figure 5: Time evolution of the energy spectra of the Goldstone excitations displayed as a function of the comoving wave number. Average over 8 runs with typical standard deviations as error bars for one of the spectra are shown. The rescaled late time spectra agree within the standard deviation in an interval $(0, k_{\text{lim}})$ which increases with time ($g = 0.1, N = 64$).

We have seen in the right end of Fig. 2 that the cooling rate of the Higgs field is nearly the same as the rate of the Goldstone field. This suggests that even if the Higgs and Goldstone components behave as completely well-defined and independent degrees of freedom as far as their dispersion relations and equations of state are concerned, they are in some sort of interaction. The situation is thermodynamically puzzling, since the kinetic temperature of the Goldstone modes is higher than that of the radial oscillations.

The investigation of the kinetic power spectra provides much more detailed information. One finds that the Higgs and inflaton degrees of freedom quickly approach classical equipartition as suggested by their EoS. The power spectra of the Goldstone degree of freedom reveal interesting regularities. Fig. 5 shows the Goldstone energy spectra at late times (well within the regime of virial equilibrium). The shape near the origin is very similar to what was found in Minkowski metric [12]. The durable deviation from equipartition appears as a result of anomalously slow relaxation in the smallest comoving k -region, frozen in an almost instant decoupling after the tachyonic instability. This is demonstrated by the fact that this part of the spectra shows perfect $a^{-4}(t)$ scaling. The scaled up power in the higher modes is gradually increasing, which apparently comes from the uniform decrease of the power of the radial motion. The k_{lim} value separating these regions is shifted gradually towards the cutoff.

The situation described above has a simple physical explanation. The massive Higgs waves can

decay into energetic pairs of elementary Goldstone modes irreversibly, even if their temperature is lower. In the language of conformally transformed variables the radial mass term scales with $a(t)$. We find $k_{\lim}(t)/a(t)$ to be approximately constant, and its value corresponds to equality in (3): $2k_{\lim}(t)a(t) \approx M_{\text{Higgs}}$. The main distinction between the two regions of Goldstone modes consists in the circumstance, that the low-(comoving)- k modes do not receive energy input from Higgs-to-Goldstone pair creation. As k_{\lim} sweeps through the Brillouin-zone completely decoupled Goldstone modes are left behind. The physics of the system becomes seriously distorted at times when $M_{\text{Higgs}}a(t)$ approaches $2k_{\text{cut-off}}$, beyond which the Higgs waves will be artificially stabilized.

6 Conclusions

In this study we focused our investigation on the very early stage of the field evolution following tachyonic instability occurring in simple realisations of the hybrid inflationary scenario. We found that the direct production of Goldstone excitations is very efficient. By a thorough analysis of the low- k part of the Goldstone spectra and its contribution to the equation of state one can separate the elementary waves from the extended objects (strings) formed from coherent Goldstone configurations. The decay of the strings can be followed through the temporal variation of the corresponding $w = p_{\text{Goldstone}}/\rho_{\text{Goldstone}}$ ratio. The smaller is the selfcoupling λ the longer the string-network lives.

We found a relatively simple model for the inflaton excitation which describes each of its Fourier modes as an independently moving elementary oscillator. By neglecting the momentum transfer between the inflaton and Higgs field we found that the oscillators are driven by the exponential growth of the radial field $\overline{r^2(t, \mathbf{x})}^V$. Simple semianalytical calculations reproduce the results of our numerical experiment as far as the inflaton field is concerned.

For the excitation of the Goldstone field, however, we could reach only a qualitative understanding. The overwhelming dominance of the kinetic energy of the radial field over its gradient energy gave a strong hint that the simplified model containing only a homogenous radial field of appropriate amplitude might account for the observed strong excitation. In case of the Goldstone motion the result of such model calculations underestimates the full numerical solution. The smaller is λ the worse is the efficiency of the excitation by the homogenous mode.

The key to the qualitative interpretation of this feature is the observation that the start of the roll-down of the radial field is not synchronous at each site. The smaller is λ the larger gradient energy is generated, already before the Goldstone excitation. The inhomogenous Higgs modes couple with similar strength to the inhomogenous Goldstone modes, like $\overline{r(t, \mathbf{x})}^V$ itself, but are much more numerous. Therefore restricting the model to the homogenous mode increasingly underestimates the strength of the Goldstone motion.

Curiously, we also found in our investigation an interesting mechanism for energetic reheating which still avoids the restoration of the symmetry. It might happen that some kind of strongly out of equilibrium dynamics (in our case the tachyonic instability) excites much more efficiently a certain degree of freedom than the order parameter. If their interaction is weak relative to the Hubble expansion rate, decoupling occurs very early and the matter field cannot climb out from the symmetry breaking minimum.

During the later transition period from radiation towards matter domination the decay of the Higgs-waves into Goldstone modes can be observed. The Fourier power spectra of the Goldstone mode is frozen gradually in a strongly out of equilibrium shape, displaying the enhancement of low- k

modes.

The features of the late time dynamics in the $O(2)$ sector, analyzed above can be summarized in a spectral variant of the system of coupled equations, which describes the variation of the energy densities contained in (radiation-like) light modes coupled to a heavy decaying degree of freedom [14]. The variation in conformal time of the comoving Goldstone mode-energies ($\rho_G(\mathbf{k})$) is affected by the decay of the Higgs waves into Goldstone particles. By the assumption that the momentum-distribution of the Higgs degree of freedom (ρ_H) obeys in each instant the equipartition rule, one conjectures the following kinetic equations in the time interval where the inequality (3) is fulfilled:

$$\begin{aligned}\frac{d}{d\eta}(\rho_G(\mathbf{k})a^4(t)) &= \Theta\left(|\mathbf{k}| - \frac{1}{2}M_{\text{Higgs}}a(t)\right)\tau^{-1}\frac{3}{4\pi}\frac{1}{k_{\text{cut-off}}^3}\rho_Ha^4(t), \\ \frac{d}{d\eta}(\rho_Ha^3(t)) &= -\left(1 - \frac{1}{8}\frac{(M_{\text{Higgs}}a(t))^3}{k_{\text{cut-off}}^3}\right)\tau^{-1}\rho_Ha^4(t)\end{aligned}\quad (13)$$

(τ^{-1} is the decay rate of the Higgs waves).

The next stage of our project is to extend the investigation to the case of gauged models of hybrid inflation [18, 21], which differs in very important aspects from the models where Goldstone modes appear.

Acknowledgements

The authors enjoyed very informative discussions with A. Jakovc and Zs. Szep. Remarks by M. Hindmarsh at SEWM'02 are gratefully acknowledged. This research was supported by the Hungarian Research Fund.

References

- [1] A.D. Linde, Phys. Rev. **D49** (1994) 748
- [2] J. Garcia-Bellido and A.D. Linde, Phys. Rev. **D57** (1998) 60557
- [3] R.L. Davis, Phys. Rev. **D32** (1985) 3172
- [4] D.N. Spergel, N. Turok, W.H. Press and B.S. Ryden, Phys. Rev. **D43** (1991) 1038
- [5] M. Yamaguchi, Phys. Rev. **D60** (1999) 103511
- [6] M. Yamaguchi, J. Yokoyama and M. Kawasaki, Phys. Rev. **D61** (2000) 061301(R)
- [7] G. Felder, J. Garcia-Bellido, P.B. Greene, L. Kofman, A.D. Linde and I. Tkachev, Phys. Rev. Lett. **87** (2001) 011601
- [8] G. Felder, L. Kofman and A.D. Linde, Phys. Rev. **D64** (2001) 123517
- [9] D. Boyanovsky, H. J. de Vega, R. Holman, D S Lee and A Singh, Phys. Rev. **D51** (1995) 4419

- [10] D. Boyanovsky, R. Holman and J. F. J. Salgado, Phys. Rev. **D54** (1996) 7570
- [11] D. Boyanovsky, D. Cormier, H. J. de Vega, R. Holman and S. Prem Kumar, Phys. Rev. **D57** (1998) 2166
- [12] Sz. Borsányi, A. Patkós and D. Sexty, Phys. Rev. **D66** (2002) 025014
- [13] M. Yamaguchi and J. Yokoyama, hep-ph/0210343
- [14] E.W. Kolb and M. Turner, *The Early Universe*, Addison-Wesley 1990, New York
- [15] T. Asaka, W. Buchmüller and L. Covi, Phys. Lett. **B510** (2001) 271
- [16] J. Garcia-Bellido, M. Garcia Perez and A. Gonzalez-Arroyo, hep-ph/0208228
- [17] Sz. Borsányi, A. Patkós and D. Sexty, hep-ph/0301117, to appear in Procs. of SEWM'02, Sept. 29-Oct. 2 2002, Heidelberg, ed. M. Schmidt
- [18] E.J. Copeland, S. Pascoli and A. Rajantie, Phys. Rev. **D65** (2002) 103517
- [19] J. Garcia-Bellido and E. Morales, Phys. Lett. **B536** (2002) 193
- [20] A.A. Grib, S.G. Mamayev and V.M. Mostapenko, Vacuum Quantum Effects in Strong Fields, Friedmann Laboratory, St. Petersburg, 1994
- [21] J. Skallerud, J. Smit and A. Tranberg, hep-ph/0210349, to appear in Procs. of SEWM'02, Sept. 29-Oct. 2 2002, Heidelberg, ed. M. Schmidt